INTERNATIONAL JOURNAL OF CIRCUITS, SYSTEMS AND SIGNAL PROCESSING
DOI: 10.46300/9106.2021.15.51 Volume 15, 2021

The Analysis of Shielding Effectiveness of the enclosure of an EMI-Filter for a Spacecraft Power Bus

Yevgeniy Zhechev, Alexander Zabolotsky
Tomsk State University of Control Systems and Radioelectronics,
40, prospect Lenina, 634050, Tomsk, 634050
Russian Federation

Received: March 27, 2021. Revised: May 6, 2021. Accepted: May 12, 2021. Published: May 18, 2021.

Abstract- In this paper, the shielding enclosure of an electromagnetic interference (EMI) filter for a spacecraft power bus was analysed for shielding effectiveness (SE). By using an electrodynamic approach, the authors conducted simulation in the frequency domain taking into account losses in the shield. The investigation covered the performance of the shielding enclosure with and without the connected cables and the influence of apertures formed between the enclosure-base and its cover. It was found that the smallest value of the SE of the enclosure is observed for the configuration with unshielded cables. However, whilst maintaining shielding integrity, attenuation of at least 88 dB in the frequency range from 0 to 20 GHz was achieved. In the study, the authors analysed the influence of printed circuit boards of EMI-filter in the shielded volume on SE of the enclosure and found that they have a weak effect on the SE. In conclusion, there is some practical guidance on the design of similar EMI-protection devices.

Keywords- Electromagnetic shielding, electromagnetic interference (EMI), spacecraft power bus, electromagnetic compatibility.

I. Introduction

During the operation of aerospace equipment (ASE), complex transient processes can occur that can generate broadband conducted and radiated electromagnetic interference (EMI). Without ensuring the required level of electromagnetic compatibility (EMC), the performance of ASE in complex electromagnetic environments is impossible [1, 2].

Shielding is the most common technology used for the protection against radiated interferences and external fields [3, 4]. Evaluating the efficiency of electromagnetic shielding is an important problem. The standards [5–7] describe methods for measuring the effectiveness of electromagnetic shielding enclosures. However, it is often difficult to conduct a full-scale experiment, so developers often use numerical simulations [8–10]. Therefore, in this paper, the authors present the results of a numerical study of the enclosure of the EMI-filter for a space-craft power bus. Previously, various studies of this object have been conducted. For example, the paper [11] presented the analysis of the cross-section of the power bus which provides electric power supply to units of the vehicle with a total power of 20 kW (Fig. 1a). The spacecraft power bus consists of input and output cables and an EMI-filter. Due to the presence of wide printed conductors and contact pads, the EMI-filter is susceptible to external fields and radiated EMI. During the operation of the spacecraft power bus, the EMI-filter is installed in a special aluminum enclosure (Fig. 1b). The authors have studied the cables of the spacecraft power bus and showed the relevance of using simulation in accordance with EMC requirements [12]. The papers [13, 14] presented the results of EMI-filter simulation in frequency and time domains. The authors also conducted an ex-

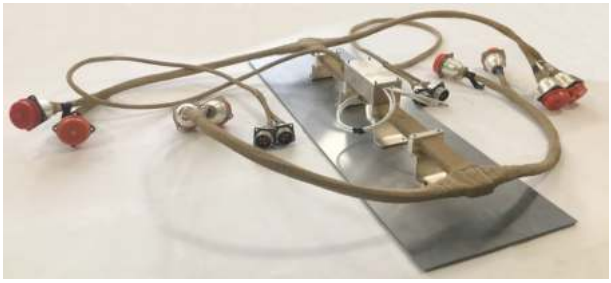

(a)

(b)

Fig. 1: Spacecraft power bus (a) and the EMI-filter in the shielding enclosure (b).

perimental study of the EMI-filter characteristics [15]. However, previously we have not analysed shielding effectiveness (SE) of the EMI-filter enclosure. There are series of approaches and methods used to analyse SE. For simple structures, the quasi-static approach [16] and analytical expressions [17, 18] are used successfully, and to analyse complex structures in a wide frequency range, the electrodynamic approach is used [19]. The paper [20] presents the experience of calculating the SE of the non-optimized simplified model of the EMI-filter enclosure using analytical expressions. The gap formed between the enclosure-base and its cover was studied as a continuous aperture of 50 μm in height. Meanwhile, the electrodynamic analysis of how actual geometrical parameters of the structure, the gap formed between the enclosure-base and its cover, as well as the connected cables influence SE have not been conducted. Thus, the purpose of this paper is to conduct such research. It is necessary to solve the following tasks: to build a 3D-model of the enclosure, to conduct electrodynamic simulation, and to analyse the obtained results.

II. Simulation Techniques and Structure

The EMI-filter is a series connection of a filter on lumped elements and a modal filter. Both devices operate in common and differential modes. The first is used to suppress low-frequency interference and the second for high-frequency interference. The modal filter also allows decomposing dangerous ultra-wideband pulses into a sequence of lower amplitude pulses. This is achieved by modal effects in the transmission line [21]. The modal filter and the filter on the lumped elements are installed inside the shielding enclosure.

The parameters of the EMI-filter enclosure after optimization (minimum weight and overall sizes) of its geometrical parameters were: 92x45x35.5 mm^3. Aluminium with electrical conductivity σ = 3.6x10^7 S/m and relative magnetic permeability μ_r = 1 was used as the enclosure material. The minimum wall thickness was 1.25 mm. Fig. 2 shows the geometrical parameters of the EMI-filter enclosure and its 3D model, as well as the influence of a plane wave on it. The Pointing vector is oriented at a right angle to the enclosure wall. The frequency of exposure varied from 0 to 20 GHz. The enclosure apertures are two rectangular holes with rounded edges, the distance between the centres of which is 10 mm, the width and height of the apertures are 8 and 4 mm, respectively. To measure field strength, 9 field monitors were located in the enclosure, with the worst SE value being analysed (Fig. 3).

At the first stage, we examined the influence of the gaps formed between the enclosure-base and its cover on the SE. This was motivated by the fact that induced high-frequency leakage currents are capable of penetrating the enclosure through these gaps under the influence of the external electromagnetic field (Fig. 4). Since the maximum tolerance (100 μm) for each part is defined in the structure of the shielding enclosure, the maximum gap can be equal to 200 μm. Therefore, this paper estimated the SE of the structure with gaps between the enclosure-base and its cover in the range from 0 to 200 μm at 50 μm intervals. Meanwhile, in the first stage, the influence of the front-face apertures was not taken into account; it was a solid metal shield, with a thickness of 2.5 mm.

At the second stage, the SE of the enclosure with open front-face apertures was studied. In addition, the

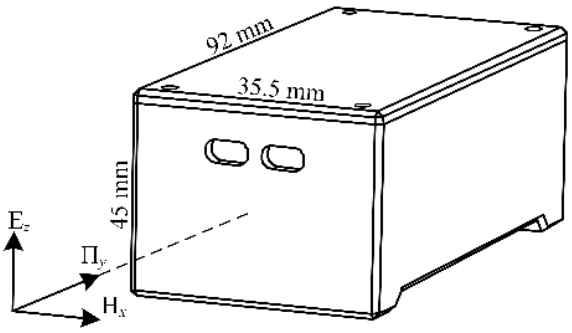

Fig. 2: Geometric parameters of the shielding enclosure and its 3D model with front-face apertures.

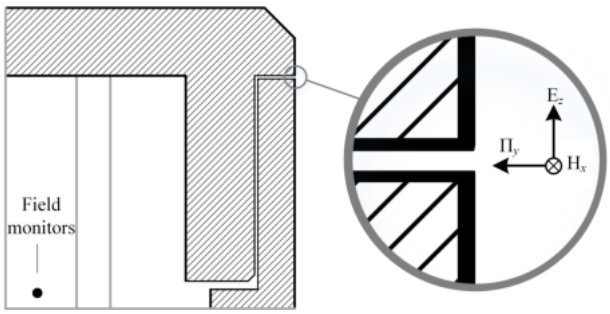

Fig. 4: Electromagnetic field penetrates through the gap formed between the enclosure-base and its cover.

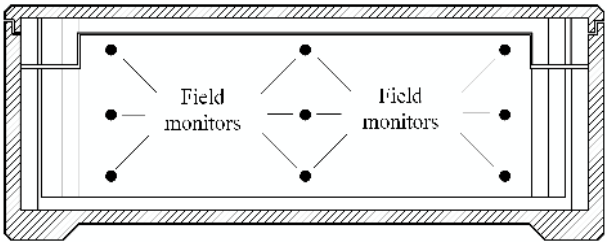

Fig. 3: Field monitors installed to measure field strength in the shielding enclosure.

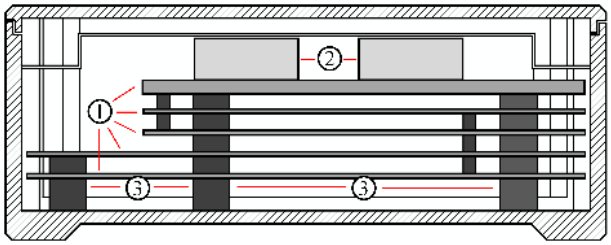

Fig. 5: Shielding enclosure with mounted PCBs, mounting screws, and toroidal cores of the EMI-filter.

Table 1: The Highest and Lowest Attenuation Values in the First Configurations Under Study

Configurations	Attenuation	
	The highest	The lowest
Without front-face apertures	143 dB	88 dB
50 μm	83 dB	43 dB
100 μm	68 dB	27 dB
150 μm	67 dB	25 dB
200 μm	66 dB	23 dB

Table 2: The Highest and Lowest Attenuation Values in the Second Configurations Under Study

Configurations	Attenuation	
	The highest	The lowest
Free apertures	65 dB	24 dB
Aperture with cable and without shield	47 dB	-5 dB
Aperture with cable and shield	152 dB	87 dB
Aperture with the cable and shifted shield	48 dB	1 dB

Table 3: The Highest and Lowest Attenuation Values in the Third Configurations Under Study

Configurations	Attenuation	
	The highest	The lowest
50 μm	83 dB	43 dB
50 μm with PCBs	89 dB	40 dB

influence of connected cables with and without a solid shield was evaluated. In each aperture, there were two copper cables of 3.2 mm in diameter and with 0.3 mm thick isolation. During operation, the contact between the enclosure-base and the solid shield can be broken because of mechanical stress. Therefore, the authors additionally simulated the enclosure with cables and a solid shield disconnected from the enclosure-base and placed at 50 μm from it. Meanwhile, at the second stage, the influence of gaps between the enclosure-base and its cover was not taken into account.

At the final stage, the SE of the shielding enclosure with the installed EMI-filter printed circuit boards (PCB) was analysed (Fig. 5). The influence of the front-face apertures was not taken into account, and the gap between the enclosure-base and its cover was 50 μm. The EMI-filter configuration consists of 5 PCBs (1). On the top layer of the first PCB, there are 3 toroidal cores (2) with $\mu_r = 300$. Six mounting screws (3) connected to the shielding enclosure pass through all PCBs. The field monitors for measuring field strength are placed both between PCBs and between PCBs and the enclosure. The worst-case attenuation was also analysed to obtain the SE in the given configuration.

III. Electrodynamic Simulation Results

Fig. 6a shows the results of the electrodynamic simulation of the shielding enclosure effectiveness which takes into account the gaps formed between the enclosure-base and its cover. The highest and lowest attenuation values in the presented configurations are summarised in Table I. The data illustrate that the highest attenuation was observed in a gap-free configuration (0 μm), whereas the lowest attenuation in the investigated frequency range was 88 dB. This result was achieved by providing shielding integrity. The configuration with a 50 μm gap showed average results. The lowest attenuation of 43 dB was observed in the frequency range from 6 to 7 GHz. It could happen because the enclosure configuration can reduce SE due to standing waves caused by resonance effects at high frequencies. As is well known, if the size of the enclosure is a divisible of the half-waves, resonances occur in it. Another cause of the reduced SE is the concentration of the electromagnetic field in the corners of the enclosure. Meanwhile, a significant decrease in attenuation was observed in configurations with a gap of 100, 150, and 200 μm. The characteristics of these configurations are similar; there are multiple resonances and fluctuations over the frequency range. The worst attenuation was observed in the 200 μm configuration (Fig. 6b), which was 23 dB. It should be noted that this result is similar to the results obtained for open front-face aperture configurations at frequencies above 8 GHz.

Fig. 7a shows the results of the electrodynamic simulation of SE of the enclosures with the open front-face apertures; with apertures and connected cables; with apertures, connected cables, and their shield. The fig-

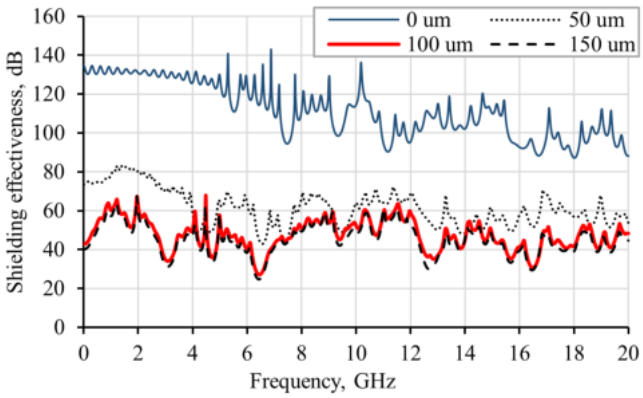

(a)

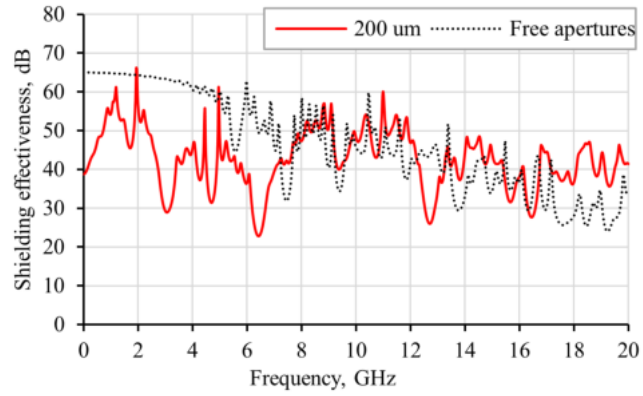

(b)

Fig. 6: SE for configurations with gaps of 0, 50, 100, 150 μm (a) and 200 μm (b).

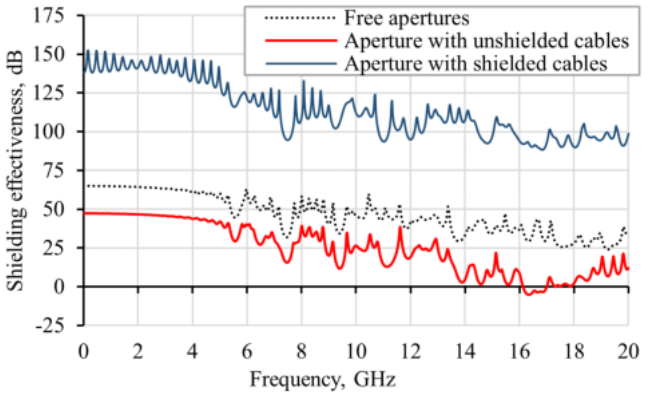

(a)

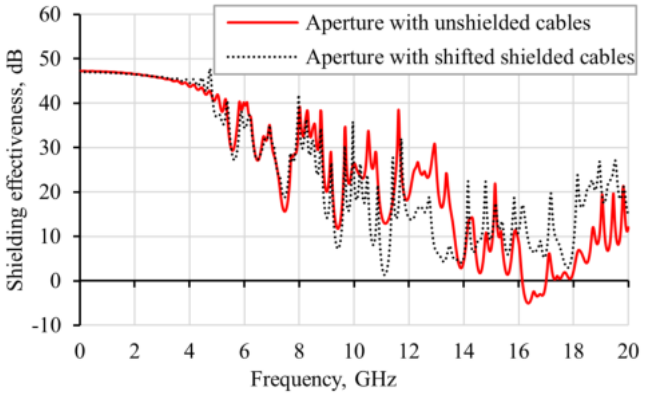

(b)

Fig. 7: SE for configurations with shielded and unshielded cables (a), as well as SE for configurations with unshielded cables and shielded cables with the shield shifted by 50 μm (b).

ure shows that the highest SE was observed in the configuration with shielded cables. The minimum attenuation in the frequency range was 87 dB. This result was achieved by eliminating open-air gaps and apertures in the shielding enclosure. It can be concluded that shielding cable wires with a thin conductive layer (50 μm for this research) can provide effective EMI protection. The results of the SE simulation of the open front-face apertures show that the overall attenuation is insignificant. At frequencies above 17.5 GHz, the SE value was reduced to 25 dB. However, the configuration with apertures and unshielded cables shows the worst results. In the frequency range from 16 to 18 GHz, there was no attenuation at all. This is explained by the fact that the radiated interference penetrates into the enclosure through the connected cables which enter the shielding volume. The overall SE level in this configuration in the full frequency range is not acceptable for most microwave applications. Fig. 7b shows the results of SE simulation of the configuration with apertures, connected cables, and the disconnected shield. It can be seen that the envelope shape in the configuration with unshielded cables and cables with shifted shield is practically the same. The formed gap significantly reduces the SE value of the shielding enclosure. Therefore when designing and mounting such devices it is critical to control the integrity of shielding boundaries. The highest and lowest attenuation values in the considered configurations are summarised in Table II.

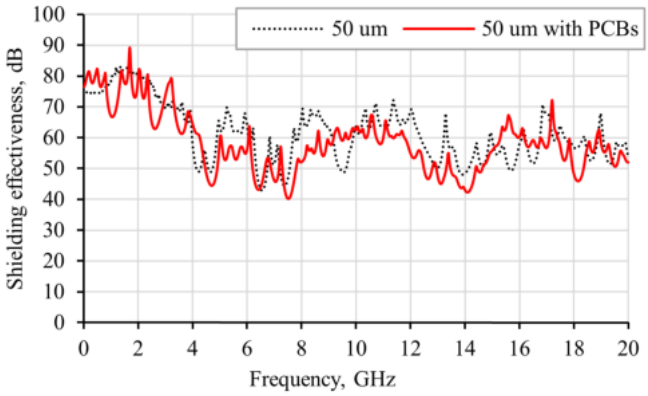

Fig. 8: SE for configurations with 50 μm gap, with PCBs and without them.

Fig. 8 shows the results of the electrodynamic simulation of the SE of the enclosure with the gap between the enclosure-base with the installed PCBs of the EMI-filter and its cover. It is observed that the SE characteristics of the enclosures with and without PCBs are similar, but they also have some differences. Due to the appearance of additional resonances caused by the interference of incident and reflected waves, the overall level of attenuation is changes. In addition, the presence of PCBs in the shielded volume shifts the resonances by frequency and amplitude. Moreover, the presence of PCBs in the shielded volume shifts the resonances by frequency and amplitude. The highest and lowest attenuation values are presented in Table III. The maximum attenuation in the configuration with installed boards changed from 83 to 89 dB and the minimum from 43 to 40 dB. However, the absolute deviation did not exceed 6 dB, which may indicate a weak influence of PCBs on the shielding enclosure effectiveness.

IV. Conclusion

Because internal and external sources increase the level of electromagnetic interference, shielding is the most effective method of providing EMC for ASE. High currents from the radiated emissions are induced on conductors and interconnections, reducing the performance of ASE. In this paper, the authors presented the results of the analysis of the SE of the spacecraft power bus EMI-filter shielding enclosure. It was found that the smallest value of the shielding enclosure SE is observed for the configuration with unshielded cables. Poor results were obtained for the configuration with the gap formed between the enclosure-base and its cover of 100-200 μm. This is due to the fact that high-frequency currents penetrate the shielded volume through the cables. However, whilst maintaining shielding integrity, attenuation of at least 88 dB in the frequency range from 0 to 20 GHz was achieved. It can be concluded that shielding cable

wires having a thin conductive layer can provide effective EMI protection. This is due to the fact that the heterogeneities that degrade the shielding integrity determine the final performance of the shielding. And in the case of thin conductive layers in the cable, the integrity of the shielding is preserved. It should be noted that the presence of PCBs in the shielded volume shifts the resonances by frequency and amplitude, but the overall effect on the SE is not significant. It should be mentioned that even using 9 field monitors, the worst SE value may still not be obtained in an enclosure in the frequency range of 0-20 GHz. To get the most accurate results, the number of monitors needs to be increased. However, a significant increase in this number can lead to large calculation costs. Furthermore, to validate the results we are planing to conduct an experimental study.

It is very important to control the impedance between the enclosure and the shield of the cables because the enclosure SE is significantly reduced. To minimize the negative impact of gaps at the connection points of the enclosure parts, it is possible to use conductive gaskets and radio-absorbing material. Other modifications of the enclosure design (internal grooves etc) makes it possible to achieve significant attenuation of radiated emissions by means of re-reflection loss. The most efficient method to provide an acceptable level of SE is still to increase the processability and accuracy of manufacturing the parts of the shielding enclosure.

Acknowledgment

The research was supported by the Ministry of Science and Higher Education of the Russian Federation (Project FEWM-2020-0041).

References

[1] R. J. Perez. Handbook of Aerospace Electromagnetic Compatibility. John Wiley & Sons, 2018.

[2] S. Celozzi, R. Araneo, and G. Lovat, "Electromagnetic Shielding," Wiley Series in Microwave and Optical Engineering, Apr. 2008.

[3] M. Ferber, R. Mrad, F. Morel, G. Pillonnet, C. Vollaire and A. Nagari, "Power efficiency and EMI attenuation optimization in filter design," IEEE Transactions on Electromagnetic Compatibility, vol.60, n.6, 2017, pp. 1811–1818.

[4] V. Rathi and V. Panwar, "Electromagnetic interference shielding analysis of conducting composites in near-and far-field region," IEEE transactions on electromagnetic compatibility, vol.60, n.6, 2017, pp. 1795–1801.

[5] I. S. Committee et al., "Ieee standard method for measuring the effectiveness of electromagnetic shielding enclosures," 1997

[6] J. D. Lee, "MIL-STD-1377 VS. MIL-STD-285 Microwave Shielding Effectiveness Measurements," 1975 IEEE International Symposium on Electromagnetic Compatibility, Oct. 1975.

[7] IEC 61000-5-7 (2001–01): Electromagnetic compatibility (EMC)—Part 5–7: Installation and mitigation guidelines: Degrees of protection provided by enclosures against electromagnetic disturbances (EM code).

[8] Y. Zhao, L. Zhao, M. Huang, Z. Li, P. Yang, J. Li, Z. Liu, Z. Li, T. Xu, D. Lu et al., "Shielding effectiveness simulation of rectangular enclosures using fit," in 2020 International Conference on Sensing, Diagnostics, Prognostics, and Control (SDPC). IEEE, 2020, pp. 317– 321.

[9] P. Xiao, P.-A. Du, and B. Zhang, "An analytical method for radiated electromagnetic and shielding effectiveness of braided coaxial cable," IEEE Transactions on Electromagnetic Compatibility, vol. 61, no. 1, pp. 121–127, 2018.

[10] X. Xu, Z. Lin, S. Wang, and S. Wu, "Effect of the rotation angle in multiring metallic meshes on shielding effectiveness," IEEE Microwave and Wireless Components Letters, vol. 30, no. 7, pp. 629–632, 2020.

[11] S. Ternov, A. Demakov, and M. Komnatnov, "Influence of the crosssection form of the power bus bar on its parameters," 2018 Moscow Workshop on Electronic and Networking Technologies (MWENT), 2018, pp. 1–4.

[12] S. Kuksenko, "Simulation of a spacecraft noise immune power network," Trudy MAI, no.105, pp. 1–20, 2019.

[13] R. Khazhibekov, A. Zabolotsky, Y. Zhechev, V. Kosteletskii, and T. Gazizov, "Development of modal filter prototype for spacecraft busbar protection against ultrashort pulses," IOP Conference Series: Materials Science and Engineering, vol.560, no.1., p. 012145.

[14] Y. Zhechev, V. Kosteletskii, A. Zabolotsky, and T. Gazizov, "Electromagnetic interference filter for spacecraft power bus," in IOP Conference Series: Materials Science and Engineering, vol.560, no.1, 2019, p. 012133.

[15] Y. S. Zhechev, V. P. Kosteletskii, and A. M. Zabolotsky, "Experimental study of a high current electromagnetic interference filter for the spacecraft power bus," Journal of Physics: Conference Series, vol. 1862, no. 1, p. 012024, Mar. 2021.

[16] A. Ivanov and M. Komnatnov, "Analytical model for estimating the shielding effectiveness of cylindrical connectors," IOP Conference Series: Materials Science and Engineering, vol.560, no.1, 2019, p. 012020.

[17] M. P. Robinson, J. Turner, D. W. Thomas, J. Dawson, M. Ganley, A. Marvin, S. Porter, T. Benson, and C. Christopoulos, "Shielding effectiveness of a rectangular enclosure with a rectangular aperture," Electronics Letters, vol.32, no.17, pp. 1559—1560, 1996.

[18] F. T. Belkacem, M. Bensetti, A.-G. Boutar, D. Moussaoui, M. Djennah, and B. Mazari, "Combined model for shielding effectiveness estimation of a metallic enclosure with apertures," IET Science, Measurement & Technology, vol.5, no.3, pp. 88—95, 2011.

[19] G. Zhang, T. Wei, J. Ding, and C. Guo, "The calculation and analysis of shielding efficiency," 2017 In-

ternational Applied Computational Electromagnetics Society Symposium (ACES), 2017, pp. 1—2.

[20] A. Ivanov, A. Kvasnikov, S. Kuksenko, and M. Komnatnov, "Software module prototype for evaluating the shielding effectiveness of radioelectronic equipment enclosures," Technologies of electromagnetic compatibility, vol.71, no.4, pp. 5—15, 2019

[21] A. T. Gazizov, A. M. Zabolotsky, and T. Rashitovich Gazizov, "UWB Pulse Decomposition in Simple Printed Structures," IEEE Transactions on Electromagnetic Compatibility, vol. 58, no. 4, pp. 1136–1142, Aug. 2016.